Dendrochronologia 90 (2025) 126300

Contents lists available at ScienceDirect

Dendrochronologia

journal homepage: www.elsevier.com/locate/dendro

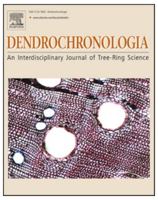

Recent declines in radial growth and wood density characterize dieback in European beech and pedunculate oak

Ester González de Andrés [a,*], Antonio Gazol [a], Michele Colangelo [a,b], Cristina Valeriano [a], Alejandro Cantero [c], J. Julio Camarero [a]

[a] *Instituto Pirenaico de Ecología (IPE-CSIC), Avda. Montañana 10005, Zaragoza 50009, Spain*
[b] *Scuola di Scienze Agrarie, Forestali, Alimentari, e Ambientali, Università della Basilicata, Potenza, Italy*
[c] *HAZI Fundazioa, Arkaute, Alava 01192, Spain*

ARTICLE INFO

Keywords:
Basal area increment
Densitometry
Drought
Fagus sylvatica
Quercus robur
Resistography

ABSTRACT

In the last decades, climate change has boosted the occurrence of severe dry and warm episodes that impair the functioning of forests. Elevated evaporative demand, i.e., high vapour pressure deficit, during the growing season limits the ability of trees to fix carbon and growth thus increasing the likelihood of tree dieback and mortality. While climate change impacts on tree growth are widely documented, we still lack a clear understanding on how wood density responds to temperature increases, particularly for hardwood tree species near their warm distribution edges. We evaluated the annual growth and wood density variability of European beech (*Fagus sylvatica* L.) and pedunculate oak (*Quercus robur* L.) in two forests suffering tree mortality in northern Spain. We used dendrochronology to quantify tree-ring-width and basal area increment (BAI) and densitometry analyses to obtain annual wood density profiles of non-declining (ND) and declining (D) trees. In addition, resistography was employed to estimate resistance drilling density. We found a higher BAI of ND as compared with D trees in the two species, since the severe 2012 drought for beech and after the 1960s for oak. By contrast, differences between vigour classes in wood density were only evident in oak during the last decade, when D trees showed a decreasing trend. Beech growth was enhanced by wet-cool summer conditions, whereas density increased in response to dry-warm spring conditions and cool temperatures during the previous autumn. Oak growth was enhanced by dry-warm conditions in the prior winter and in the summer of the year of growth. High minimum temperatures during the previous autumn, spring and summer increased wood density in ND oak trees, while high precipitation during spring reduced wood density in D trees. We found that resistance drilling profiles did not differ between vigour classes in beech, but D oak trees showed lower resistance to penetration in the sapwood than ND trees, consistent with densitometry profiles. Our results indicate that radial growth data have better capacity to differentiate declining and healthy trees than density and resistograph profiles in European beech and pedunculate oak.

1. Introduction

Rising temperatures due to climate change and accompanied increases in vapor pressure deficit and a higher frequency and intensity of droughts reduces the length of the growing season (Rahmati et al., 2023), alters canopy temperature regulation (Gauthey et al., 2024), leads to declines in photosynthesis and growth rates (Grossiord et al., 2020) and increase the likelihood of tree mortality (Senf et al., 2020). There is thus an urgent need for understanding how environmental conditions affect the performance of tree species to better forecast forest dieback and mortality (Camarero et al., 2015; Hartmann et al., 2022). Mortality hotspots, i.e., those forests that shows excess (much higher than basal rates) of tree mortality (Allen et al., 2010, 2015; Senf et al., 2020; Hammond et al., 2022), are useful natural laboratories to study differences between coexisting healthy and declining trees (Hartmann et al., 2018). Here, we follow a multi-proxy approach to advance in this research gap by studying temporal trends in radial growth and wood density of healthy and declining European beech (*Fagus sylvatica* L.) and

---

[*] Corresponding author.
E-mail addresses: ester.gonzalez@ipe.csic.es (E. González de Andrés), agazol@ipe.csic.es (A. Gazol), michele.colangelo@unibas.it (M. Colangelo), cvaleriano@ipe.csic.es (C. Valeriano), acantero@hazi.eus (A. Cantero), jjcamarero@ipe.csic.es (J.J. Camarero).

https://doi.org/10.1016/j.dendro.2025.126300
Received 20 September 2024; Received in revised form 17 January 2025; Accepted 6 February 2025

Pedunculate oak (*Quercus robur* L.) trees in two mortality hotspots near the warm distribution limits of the species in northern Spain (Camarero et al., 2021).

European beech and pedunculate oak are two deciduous broadleaved species widely distributed in Europe with an important ecological and economical value (Eaton et al., 2016; Houston Durrant et al., 2016). Empirical evidence indicates that the xylogenesis (i.e., wood formation) and growth of the two species is sensitive to drought (van der Werf et al., 2007; Skiadaresis et al., 2019; Serra-Maluquer et al., 2019; Bose et al., 2021; Jiang et al., 2024), although comparative studies in central Europe indicate that oak tolerates drought better than beech in different environments (Scharnweber et al., 2013; Vitasse et al., 2019; Vanhellemont et al., 2019; Meyer et al., 2020; Enderle et al., 2024). This different drought sensitivity has been related to differences in stomatal regulation strategies, depth of root systems or wood anatomical traits (Klein, 2014; Meyer et al., 2020; Kahmen et al., 2022). Nevertheless, dieback and mortality events of both species have been reported in different regions, mainly attributed to the effect of hotter droughts in the case of beech (Leuschner, 2020; Camarero et al., 2021; Rohner et al., 2021; Frei et al., 2022; Martinez del Castillo et al., 2022) and to the interaction between climate change and biotic factors in the case of oaks (Drobyshev et al., 2007; Losseau et al., 2020; Macháčová et al., 2022; Kowsari and Karimi, 2023). It remains unclear how the distribution of the two species will change in response to climate change, particularly near their warmer southern distribution limits (Dyderski et al., 2018), where local studies can help to calibrate distribution models (Hartmann et al., 2022).

Within mortality hotspots, a reduced capacity to resume growth after drought will result in lower growth rates and more negative growth trajectories in declining than in healthy trees (Helama et al., 2009; DeSoto et al., 2020). Besides, these changes can be accompanied by a higher response of growth variability to climate in declining trees (e.g., Camarero et al., 2018, 2021). These divergent responses between coexisting trees can help attributing potential climatic stressors triggering forest decline. In this respect, dendrochronology allows the reconstruction of past and current growth patterns, thereby allowing to identify different growth trajectories and growth responses to climate of coexisting trees (Camarero et al., 2015; Cailleret et al., 2018; DeSoto et al., 2020). However, ring-width variations do not fully capture the complex responses of tree performance to climate variations and the use of additional wood traits can provide further insights (Skomarkova et al., 2006; Süßel and Brüggemann, 2021; Giberti et al., 2023; Olano et al., 2023; Minikaev et al., 2024). For instance, López et al. (2021) showed that differences in latewood density between declining and non-declining Canarian pine (*Pinus canariensis* C.Sm.) trees started before the differences in ring-width suggesting larger carbon limitations in declining trees. In hardwood tree species, wood density depends on the size, wall-thickness and abundance of vessels and fibers, thus responding to different environmental and climatic variables than ring-width (Skomarkova et al., 2006; Toigo et al., 2015). Previous studies have reported positive correlations between wood density and temperature and water deficit during summer in both ring-porous and diffuse porous species (Bergès et al., 2008; Peters et al., 2020). Therefore, temporal variations in wood density can offer valuable information to determine divergent responses between non-declining and declining beech and oak trees (van der Werf et al., 2007; Bytebier et al., 2022). However, information related to wood density changes in dieback and mortality processes in hardwood tree species is still scarce (but see Soheili at al., 2021). This fact is partly related to challenges posed by hardwood species to measure wood density resulting from diverse anatomical structures such as varying vessel sizes and fiber distribution (Diaconu et al., 2016)

Here, we used dendrochronology and densitometry to reconstruct the growth and wood density trajectories of healthy and declining European beech and pedunculate oak in two mortality hotspots near the warmer edge of the species distribution limits (see Camarero et al., 2021). Additionally, we explored the use of non-destructive resistography to test for differences in resistance drilling density between non-declining and declining trees (Gao et al., 2017; Fundova et al., 2018). Our specific objectives were 1) to determine whether declining and healthy trees show differences in their radial growth and wood density profiles; 2) to establish the relationships of climatic conditions with growth and wood density; and 3) to evaluate the relationships between the different proxies of tree performance. We expected 1) different climatic associations of growth and wood density due to partial decoupling of their variabilities, as they depend on different processes during xylogenesis. As a result, wood density would be more dependent on climatic conditions during the growing season of the current year (Čufar et al., 2008; Skomarkova et al., 2006; Toigo et al., 2015), while ring-width might also depend on the prior-year climate conditions (van der Werf et al., 2007). Along this, we also expected 2) differences in the year-to-year response of wood density variability to climate between species giving that they have different wood anatomical properties, growth characteristics and strategies to withstand drought (Fabiani et al., 2022). Finally, we expected 3) negative relationships between growth and density since faster growth would involve wider vessels so softer wood and less resistance too penetration (Chave et al., 2009).

2. Material and methods

2.1. Study sites and tree species

The study area is located in Araba, Basque Country, northern Spain. We studied two forest stands undergoing canopy dieback, one stand in Opakua dominated by *Fagus sylvatica*, and one stand in Beluntza dominated by *Quercus robur*. The understory of Opakua is dominated by *Juniperus communis* L., *Prunus spinosa* L. and *Rosa canina* L. Soils are thin and developed on limestone. Other woody species present in the Beluntza site are *Corylus avellana* L., *Crataegus monogyna* Jacq, *Ilex aquifolium* L., and *Hedera helix* L. At this relatively flat site, the deep, well-developed clay soils can become waterlogged in winter and dry in summer.

Climatic conditions are mild and temperate at the study sites (Fig. S1). Monthly maximum and minimum temperature and total precipitation for the period 1950–2020 were obtained from the 0.25º gridded E- OBS v. 26.0e database (Cornes et al., 2018). The coldest and warmest months are January (4.2º C) and July-August (18.5º C), respectively. The month with the highest rainfall is November and the driest months are July and August. In addition, the Standardized Precipitation Evapotranspiration Index (SPEI) was used to describe drought severity (Vicente-Serrano et al., 2010). This is a normalized multiscale drought index based on the cumulative difference between precipitation and potential evapotranspiration. SPEI data for each study site were downloaded from the 1.1-km^2 gridded series of the Spanish SPEI database (Vicente-Serrano et al., 2017).

2.2. Field sampling and dendrochronological methods

At each study site, we sampled pairs of dominant non-declining (ND) and declining (D) trees randomly distributed within the stands. In total, 60 trees were sampled 30 European beech trees and 30 pedunculate oak trees. Tree vigour classes were established based on defoliation estimated by visual assessment of crown transparency (Dobbertin, 2005). We selected the trees based on their recent defoliation levels by considering neighbouring individuals showing high (>60 %, D trees) or low (<40 %, ND trees) canopy defoliation, respectively. Defoliation was assessed during late spring-early summer and trees were labelled based on their contrasting defoliation status. For each selected tree, diameter at breast height (DBH) and tree height were measured using tapes and a laser rangefinder (Nikon, Forestry Pro II), respectively. Sampling was conducted during November 2020 and January 2018 in beech and oak stands, respectively. For the sake of simplicity, the end of the study period for both species will be named 2019, although the last ring for beech trees is 2020 and 2017 for oaks.

Annual growth of selected trees was evaluated using dendrochronology. Two cores at 1.3 m height were extracted from each tree, perpendicular to the maximum slope, using 5-mm Pressler increment borers (Haglöf, Sweden). Cores were air-dried, glued onto wooden mounts and sanded until tree rings were clearly visible (Fritts, 2001). All samples were visually cross-dated, and tree-ring width (TRW) was measured with a 0.001 resolution using scanned images (resolution 2400 dpi) and the CooRecorder-CDendro software (v. 9.8.1, Saltsjöbaden, Sweden) (Maxwell and Larsson, 2021). The quality of cross-dating was checked using the COFECHA software, which calculates moving correlations between individual series of ring-width values and the mean sites chronologies (Holmes, 1983).

Each individual TRW series was detrended by fitting cubic-smoothing spline curves of 30 years with a 50 %-frequency response cut-off. This procedure preserved high-frequency variability potentially related to climate and minimize the influence of biological trends or disturbance effects (Cook and Kairiukstis, 1990). Then, autoregressive models were applied to remove the first-order autocorrelation in detrended series and generate series of residual ring-width indices (RWIres). Finally, a biweight robust mean was computed to produce chronologies for each species and vigour class. Dendrochronological statistics were calculated over the best-replicated period (1950–2019) including the first-order autocorrelation (AC), the Expressed Population Signal (EPS), mean sensitivity (MS) and mean correlation among indexed ring-width series for each species in each site (*Rbar*) (Briffa and Jones, 1990; Wigley et al., 1984).

Additionally, individual TRW series were transformed to basal area increment (BAI). BAI is an accurate indicator of tree vigour and absolute accumulated growth because it accounts for the variation caused by adding volume to a circular stem (Biondi and Qeadan, 2008). BAI series were calculated using the following equation and assuming concentric rings:

$$\mathrm{BAI} = \pi\,(\mathrm{R}_t^2 - \mathrm{R}^2{}_{t-1}) \tag{1}$$

where R_t^2 and $\mathrm{R}^2{}_{t-1}$ are the radii corresponding to the current (t) and prior ($t-1$) years, respectively. All the tree-ring width processing and statistics calculation were performed using the package *dplR* (Bunn et al., 2020) in R software (R core Team, 2023).

2.3. Densitometry analysis

For the densitometry analyses, we extracted an additional core from 23 beech trees (13 ND trees and 12 ND trees) and 16 oak trees (8 ND trees and 8 ND trees) using a 10-mm Pressler increment borer (Haglöf, Sweden). The wood samples were air dried and glued on wooden mounts. For each core, thin 1.2-mm-thick slices were cut with a double-blade saw. The slices were then radiographed on an Itrax Multiscanner (Cox Analytical Systems, Sweeden) at the CETEMAS laboratory (Asturias, Spain). The Multiscanner, equipped with a Cu-tube (Bergsten et al., 2001), was operated at 30KV and 50 mA, with an exposure of 25 s at each sample point and a step size of 20 μm (Moreno-Fernández et al., 2018). The radiographic images obtained from the Itrax Multiscanner were analyzed in WinDENDRO (Regent Instruments, Canada) to determine wood density values for each point in the wood sample. This allowed us to define wood density profiles and to determine mean tree-ring density (TRD) series. Cross-dating was again performed using the COFECHA software (Holmes, 1983). Tree-ring density series were detrended using a cubic spline of 30 years with a 50 %-frequency response cut-off and first-order autocorrelation was removed by fitting autoregressive models to obtain residual ring-density indices (RDIres). RDIres were averaged by species and vigour classes by using biweight robust means.

We additionally conducted the non-destructive measurements of resistance drilling as a proxy of variation in wood density (Gao et al., 2017). For that purpose, we used the IML-RESI PD500 (Instrumenta Mechanik Labor, Germany) and Resistograph R650-SC (Rinntech, Germany) resistance borers in the case of beach and oak, respectively. These resistance borers drive a 3-mm-diameter needle through the tree and measure the resistance to turning of the spade bit at regular intervals. The IML-Resi and the Resistograph devices differ in the measure provided, which are relative amplitude in a scale from 0 % to 100 % and resistance drilling density, respectively. Drilling was conducted bark-to-bark if possible, through the pith of the tree, except when trees had a DBH greater than 50 cm due to methodological limitations. Resistance drilling profiles were trimmed to exclude the bark and determine the point of approximate cambium. This point corresponded approximately to the first 2 and 3 cm for beech and oak trees, respectively, due to the difference in bark thickness between the two species (Kattge et al., 2020).

2.4. Statistical analyses

We tested for differences in mean tree values (tree size, ring-width and wood density measures) between vigour classes using one-way ANOVA tests. Differences between ND and D trees and trends of radial growth (BAI), wood density and resistance drilling series in the two species were evaluated by fitting linear mixed-effects models (LMMs, Pinherio and Bates, 2000). Vigour class, calendar year (distance from the bark to the pith, that is depth, in the case of resistance to penetration) and their interaction were regarded as fixed effects. Models also included random intercepts associated with tree identity and year to account for unspecified tree-, and year-level factors (Mehtätalo et al., 2011). Growth and wood density models were restricted to the period 1950–2019. Response variables were transformed ($\log[x + 1]$) to fulfil normality and variance homogeneity assumptions. LMMs were fitted using the *lme4* and *lmerTest* packages (Bater et al., 2015; Kuznetsova et al., 2017). Estimates and confidence limits of LMMs were calculated using the *emmeans* package (Lenth, 2023). In addition, we further evaluated whether the BAI, wood density and resistance drilling series differed among tree vigour classes at each time or spatial step for each species using the Wilcoxon rank sum test.

Climate – growth relationships were assessed by calculating bootstrapped correlations between RWIres and monthly maximum and minimum temperature, total precipitation and drought severity (SPEI). The window of analysis spanned from previous September to September of the year of tree- ring formation during the period 1950–2019, when EPS > 0.85 (Table 1). Correlations with SPEI were performed at the 1-, 3-, 6-, 9- and 12-month time scale. To assess the temporal stability between growth indices and selected SPEI index, we calculated 20-year moving correlations between these series. The same procedure was followed to evaluate wood density (RDIres) associations with climate. Relationships with climate were assessed using the R package *treeclim* (Zang and Biondi, 2015).

We modelled growth, wood density and resistance drilling of ND and D trees using generalized additive mixed models (GAMMs; Wood, 2017). For each study species, we adjusted individual BAI and wood density as a function of calendar year, and resistance drilling as a function of distance from cambium, using thin-plate regression splines with a maximum of five degrees of freedom (Wood, 2003). To account for growth and density divergences between ND and D trees we also considered interactions between calendar year or distance from cambium and vigour class. To consider ontogenetic changes in tree size, DBH was included as a fixed factor. We also included tree identity as a random effect, since series are repeated measures over the same individual, and a first- order autocorrelation structure to account for dependency of growth in year t on the growth of the previous year. The GAMMs were fitted using the R package *mgcv* (Wood, 2011).

Finally, we evaluated the relationships between radial growth and density proxies considering both temporal and inter-tree variability

Table 1

Characteristics (mean ± standard error) of sampled sites and trees. Different letters indicate significant differences ($p < 0.05$) between tree vigour classes according to one-way ANOVA tests.

	Fagus sylvatica		*Quercus robur*	
	ND trees	**D trees**	**ND trees**	**D trees**
Latitude N (°)	42° 47’ 58”		42° 57’ 06”	
Longitude W (°)	2° 19’ 52”		2° 53’ 25”	
Elevation (m a.s.l.)	1020		610	
MAT (°C)	10.88 ± 0.08		11.03 ± 0.08	
MAP (mm)	830 ± 15		790 ± 18	
No. trees (no. radii)	15 (27)	15 (30)	15 (31)	15 (29)
DBH (cm)	40.73 ± 1.98a	41.02 ± 1.89a	53.73 ± 2.32a	45.34 ± 1.94b
Tree height (m)	17.9 ± 0.4a	14.8 ± 0.3b	27.1 ± 0.8a	23.8 ± 0.6b
Tree age at 1.3 m (years)	110 ± 7a	98 ± 5a	140 ± 7a	147 ± 4a
TRW (mm)[a]	1.26 ± 0.13a	1.29 ± 0.06a	1.13 ± 0.07a	0.57 ± 0.04b
AC[a]	0.64 ± 0.03a	0.59 ± 0.03a	0.48 ± 0.03a	0.73 ± 0.02b
Rbar[a]	0.473	0.457	0.411	0.290
MS[a]	0.289	0.319	0.236	0.241
EPS[a]	0.921	0.927	0.913	0.861

Abbreviations: non-declining (ND) and declining (D) trees, mean annual temperature (MAT), mean annual precipitation (MAP), diameter at breast height (DBH), tree-ring width (TRW), first-order autocorrelation (AC), mean inter-series correlation (*Rbar*), mean sensitivity (MS) and Expressed Population Signal (EPS).

[a] Calculated for the period 1950–2019 on raw (TRW, AC) or standardized (*Rbar*, MS, EPS) ring-width values.

within each species. To analyse associations over time, tree-level RWIres was fitted against RDIres and its interaction with tree vigour class. Tree identity was regarded as random factor to account for repetitions within each tree. To assess the relationship among individuals, we calculated Pearson correlations between the mean values of BAI, wood density and resistance drilling at tree level. BAI and wood density were averaged over the period 1950–2019, whereas resistance drilling included the first 20 cm from the cambium.

3. Results

We found that ND trees were taller (both species) and had thicker stems (only oak) than D trees (Table 1). Radial growth (BAI) differed between vigour classes (Fig. 1). In beech, ND trees grew significantly more than D trees during 2012–2020 and an abrupt growth reduction was found in the period 2003–2006 pointing to the 2003 and 2012 droughts (Fig. S1c) as factors triggering the decline of D trees. This period was much longer in the case of oak since the significant difference between ND and D trees began in 1960, thus pointing to other factors than recent droughts. Trends of BAI during the period 1950–2019 also differed between vigour classes of both species (Table 2). For beech, growth of ND trees showed a positive trend but not D trees. For oak, growth of ND trees had a positive trend and growth of D trees had a negative trend (Fig. 1).

Significant bootstrapped correlations between residual ring-width indices (RWIres) and climate variables differed between species. Beech trees had a negative response to July maximum temperature and positive to June precipitation. The negative response to July maximum temperature was larger, in absolute terms, for ND than for D trees. Previous September maximum (D trees) and minimum (ND trees) temperature also had a negative relationship with beech growth indices (Fig. 2**a**). Meanwhile, maximum temperatures did not show significant relationships with growth of oak trees, but minimum temperature showed negative correlations during the previous February and positive correlations during May and July. Only D oak trees negatively responded to January minimum temperature and precipitation (Fig. 2**b**). Thus, the results suggest that summer water scarcity (June) and heat (July) limit the growth of beech. These results are supported by the SPEI-RWIres correlations, which were highest with the 3-month scale index from July, particularly at the end of the period, but with no differences between vigour classes (Fig. S2a). Meanwhile oak growth is mainly limited by cold and wet prior-winter conditions as shown by the lack of significance with the drought index (Fig. S2b).

Tree-ring wood density in both vigour classes of beech trees was not significantly different throughout the study period (Fig. 3**a**). Wood density of oak trees was similar between vigour classes for much of the study period but beginning in the early 1980s the density of D trees separated from that of ND trees and was eventually significantly lower during the last few years (2011–2017) (Fig. 3**b**). All tree-ring density series showed negative time trends, and such negative trend was more pronounced in the D trees than in ND trees of oak (Table 2; Fig. 3). Thus, these results confirm that wood density increases from bark to pith and that the divergences in wood density between D and ND trees are decoupled from separations in ring-width.

Contrasting results were found regarding correlations between climate variables and ring-density indices (RDIres). On one hand, density of beech positively responded to March (ND and D trees) and June (ND trees) maximum temperature, and negatively to previous October maximum (ND trees) and minimum (ND and D trees) temperature and March (ND and D trees) precipitation (Fig. 4**a**). Only beech D trees showed a negative correlation with previous November precipitation and April minimum temperatures. Consistently, the strongest correlations with SPEI were found at 3-month scale of March. Similar to growth, density-water availability correlations were enhanced from the mid-1990s onwards, showing no differences between ND and D trees (**Fig, S3a**). On the other hand, density of ND trees of Q. *robur* showed positive associations with minimum temperature of previous November, May and July, while April precipitation was positively related to density of D trees (Fig. 4**b**). Only oak D trees showed a negative response to July maximum temperatures. No significant correlations were found between drought index and oak wood density (Fig. S3b). These results suggest that early spring and previous autumn climate conditions drive wood density variability in beech, while in oak summer temperatures and precipitation seem to be important.

The results of the LMMs relating the resistance to penetration with drilling depth showed that resistance increased with depth with no differences between ND and D trees in both species (Fig. 5; Table 2). Along the penetration depth, we found no differences between vigour classes of beech. However, the first three centimetres of D oak trees showed less resistance to penetration than ND oak trees. This result agrees with that of wood density measurements obtained by destructive methods (Fig. 3).

The results of the GAMMs are consistent with what has been presented so far (Fig. 6). Differences in growth trends between ND and D trees were very noticeable since early 2000s and 1990s in beech and oak, respectively. In contrast, differences in trends of tree-ring density were less evident. The only noticeable difference between vigour classes in the resistance drilling was found in the first centimetres of the oak wood profiles. The largest percentage of variation was explained in oak BAI, but the lowest percentage corresponded to oak wood density, suggesting that density trends vary considerably between D individuals in this species. Resistance drilling models explained higher percentages of variation pointing to the lower sensitivity of these methodologies to capture inter-individual variability (Table 3).

We found that residual series of ring-width and ring-density were positively related irrespective of the vigour class in the two study species (Table 4). At the individual tree level, no significant relationships were

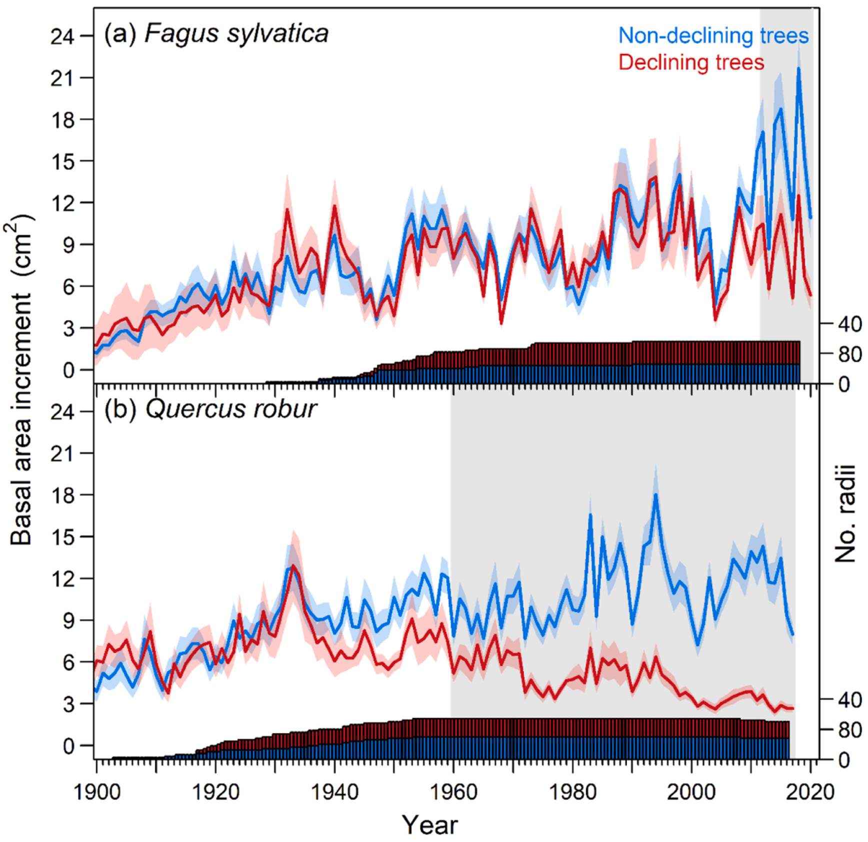

Fig. 1. Interannual variation of basal area increment (BAI) of non-declining (blue lines) and declining trees (red lines) of European beech (*Fagus sylvatica*, **a**) and pedunculate oak (*Quercus robur*, **b**). Solid lines represent the means and shaded areas around them the standard error of the mean. The bars show the annual number of measured radii (right y axes) at each site. The grey filled areas indicate the periods when BAI of tree vigour classes significantly ($p < 0.05$) differed according to Wilcoxon rank- sum tests.

Table 2

Linear mixed-effects models characterizing trends of growth, wood density and resistance drilling as a function of the tree vigour class of the study species. Growth and densitometry profiles are fitted against year and resistograph profiles against distance from the bark to the pith (i.e., depth). For each variable, the *F*-statistic and its associated *p*-value are shown.

		Fagus sylvatica		***Quercus robur***	
		F-statistic	*p*-value	*F*-statistic	*p*-value
BAI	Year	10.110	0.002	20.908	< 0.001
	Vigour class	0.572	0.456	33.245	< 0.001
	Year x class	73.764	< 0.001	510.01	< 0.001
Wood density	Year	509.62	< 0.001	39.679	< 0.001
	Vigour class	0.002	0.962	1.835	0.197
	Year x class	2.090	0.291	15.973	< 0.001
Resistance drilling	Depth	122.12	< 0.001	662.84	< 0.001
	Vigour class	1.850	0.185	0.130	0.7213
	Depth x class	0.166	0.684	2.933	0.087

found between BAI and wood density (period 1950–2019) for either beech ($r = -0.13$; $p = 0.56$) or oak ($r = -0.07$; $p = 0.79$). For beech, we found that those trees that presented greater average BAI values in the period 1950–2019 were less resistant to penetration ($r = -0.56$; $p < 0.05$), while this relationship was marginally significant in the case of oak ($r = -0.43$; $p = 0.09$). Destructive and non-destructive density measurements were positive related in beech ($r = 0.44$; $p = 0.03$) but not in oak ($r = 0.22$; $p = 0.41$). We found no differences in BAI, density profile or resistance to penetration averaged at the tree-level between ND and D beech individuals (Fig. S4a). In the case of oak, ND trees showed higher BAI values (period 1950–2017) than D trees, whereas no significant differences were found in the average values per tree of wood density (period 1950–2017) or resistance drilling density (0.00–20.00 cm depth) (Fig. S4b).

4. Discussion

The so-called multi-proxy approach can provide a better understanding of the factors affecting tree performance (Skomarkova et al., 2006; Colangelo et al., 2017; Süßel and Brüggemann, 2021; Giberti et al., 2023; Olano et al., 2023; Minikaev et al., 2024). To our knowledge, this is the first study comparing the wood density profiles of declining (D) and non-declining (ND) trees of temperate hardwood species, despite several studies have examined year-to-year variations in density records of beech (Skomarkova et al., 2006; Peters et al., 2020; Bytebier et al., 2022) and oak species (Bergès et al., 2008; Diaconu et al., 2016). Particularly, we found that year-to-year variability in ring-width and wood density depends on different climatic parameters (Bergès et al., 2008; van der Werf et al., 2007; Bytebier et al., 2022). This study provides evidence of more conspicuous divergence between D and ND trees in the case for long-term growth series (BAI), in agreement with previous studies (Camarero et al., 2021), than those of wood density profiles.

We found clear divergences in growth trajectories between vigour classes but with different duration in the two species studied (Fig. 1), as previously reported (Camarero et al., 2021). The onset of European beech decline coincided with a strong growth reduction in 2003, which is regarded as an important drought at the continental scale (van der Werf et al., 2007), and the severe impact of the 2012 drought which was important in Spain (Gazol et al., 2018). The occurrence of severe

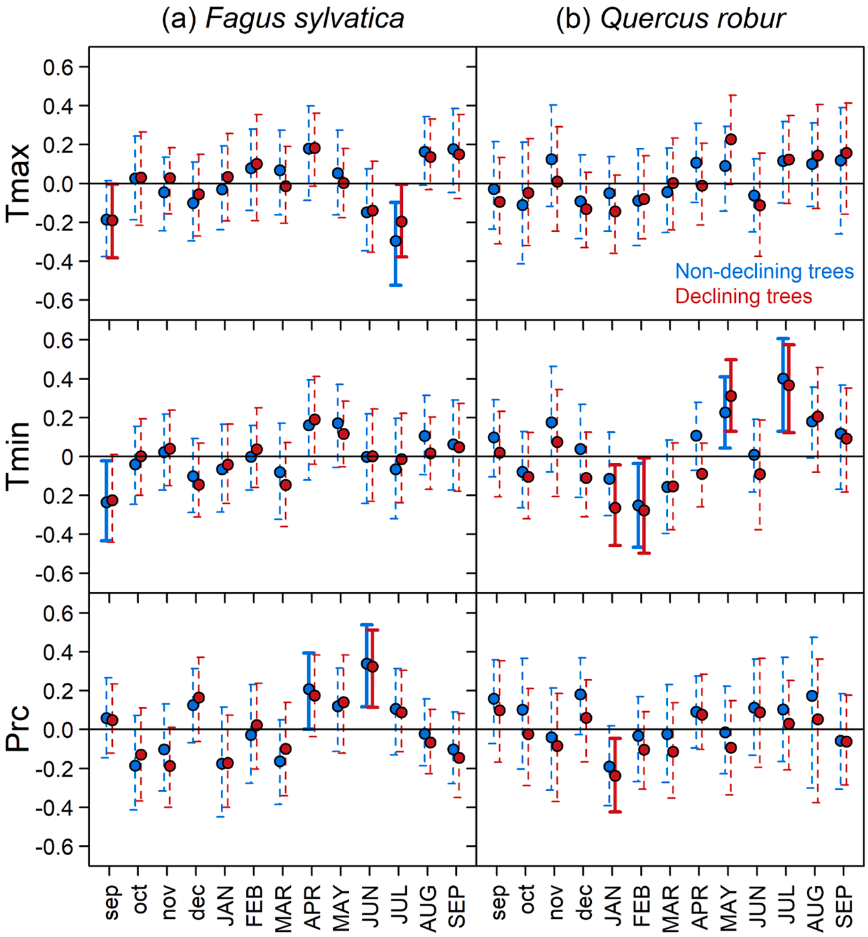

Fig. 2. Bootstrapped correlations between residual ring-width indices (RWIres) and monthly maximum temperature (Tmax), minimum temperature (Tmin) and precipitation (Prc) of European beech (*Fagus sylvatica*, **a**) and pedunculate oak (*Quercus robur*, **b**). Symbols with continuous error bars are significant ($p < 0.05$).

droughts has been also related to growth decline and dieback processes of pedunculate oak (Drobyshev et al., 2007; Skiadaresis et al., 2019). For example, Süßel and Brüggemann (2021) found that the 2018 drought reduced the formation of late wood in year 2019 by decreasing the amount of starch reserves. However, the separation between ND and D oak trees backs to the early 1960s points to additional factors than drought triggering the dieback. Camarero et al. (2021) attributed this decline to the occurrence of a severe cold spell at the early 1970s, in line with other studies (Matisons et al., 2013; Losseau et al., 2020). For instance, Matisons et al. (2013) found that vessel lumen area of pedunculate oak in Latvia showed divergent trajectories between regions after the 1979 cold year. In any case, caution is required as beech and oak trees were not sampled in the same site which difficulties the comparison. In fact, the Beluntza site is partially waterlogged and pedunculate oak is sensitive to changes in the water table depth (Gričar et al., 2013; Skiadaresis et al., 2019), which can also interact with cold stress and soil conditions (Helama et al., 2009; Rozas and García-González, 2012). Furthermore, the low growth rates of D oak trees could also show the predisposition of this tree class to dieback (Cailleret et al., 2017).

Wood density variability did not differ between vigour classes of beech, but D oak trees showed lower values and more negative trends of wood density than ND trees during the last decades (Fig. 3). These results are in line with some of the findings of previous research analysing density and wood anatomy in Persian oak (*Quercus brantii* L.; Soheili et al., 2021). Those authors reported that D oak trees presented higher wood density, narrower rings, smaller vessel lumen area and more tyloses than ND trees (Soheili et al., 2021). Wood density of pedunculate oak has been found to be directly proportional to the latewood density which increased as the percentage of area occupied by vessels decreased (Rao et al., 1997). Furthermore, D oak trees tend to grow less and also form narrow earlywood vessels than ND trees (Colangelo et al., 2017), thereby having a lower potential hydraulic conductivity (Tulik, 2014). The differences in wood density between vigour classes of oak trees but not beech trees can be related to the higher variability of wood density in the ring-porous oak compared to diffuse-porous beech due to anatomical and physiological differences between these two functional groups (Yin et al., 2023). The long-term radial growth divergence between ND and D oak trees, which is restricted to the later years in the case of beech trees, may also influence wood density profiles considering the lag period that apparently exists between the response of both variables during the dieback. Interestingly, the recent reduction of wood density observed in both species, which agrees with the general trend found in European forests (Pretzsch et al., 2018, but see Torresan et al., 2024), could be also viewed as an acclimation response because it would allow increasing wood water storage (hydraulic capacitance) and partially alleviate drought stress (Santiago et al., 2004). However, a decline in wood density would correspond to a reduction in carbon uptake and thus question the climate-warming mitigation potential of the affected forests (Pretzsch et al., 2018).

Generally, tree species with high growth rates are associated with lower wood density (Chave et al., 2009). However, translating this interspecific pattern to intraspecific scales is complex and has yielded less conclusive results. Although some studies were not able to detect significant associations between ring-width and wood density in hardwood species (e.g., Fajardo, 2018; Arnič et al., 2022), a positive

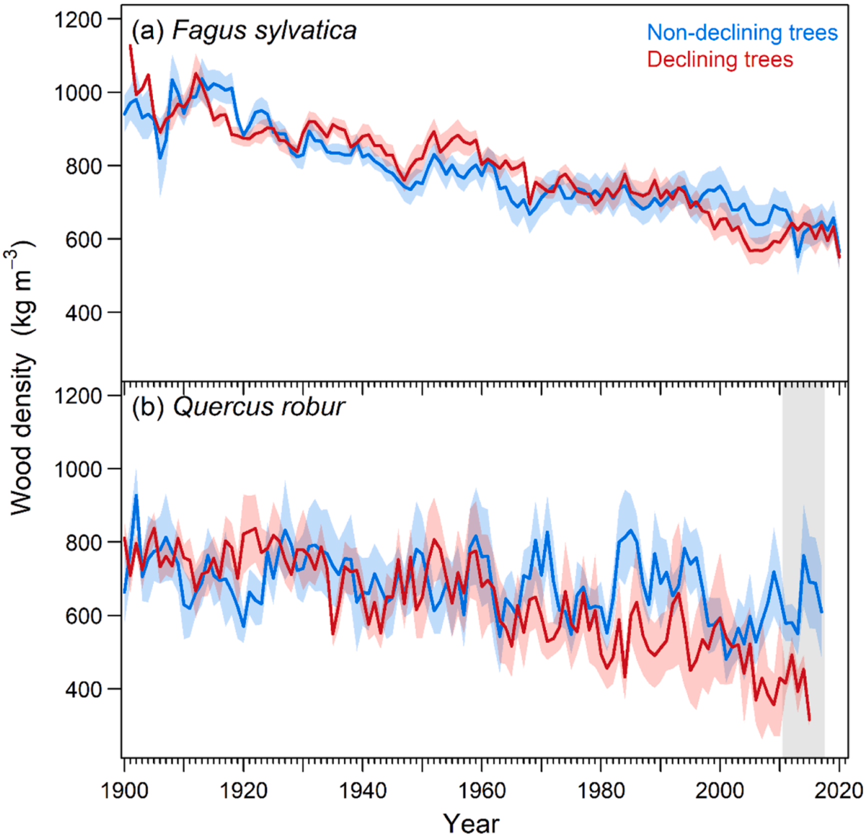

Fig. 3. Interannual variation of tree-ring wood density of non-declining (blue lines) and declining trees (red lines) of European beech (*Fagus sylvatica*, **a**) and pedunculate oak (*Quercus robur*, **b**). Solid lines represent the means and shaded areas around them the standard error of the mean. The grey filled areas indicate the periods when wood density of tree vigour classes significantly ($p < 0.05$) differed according to Wilcoxon rank- sum tests.

relationship has been reported in beech (Bontemps et al., 2013; Diaconu et al., 2016; Peters et al., 2020) and oak species (Bergès et al., 2008; Delpierre et al., 2016). Consistently, we have found that year-to-year variations of radial growth positively correlated with wood density in both species (Table 4). Indeed, Peters et al. (2020) found that variability in wood density of beech was mainly controlled by variations in the size and number of vessels and the proportion of fibres, so that vessel density decreases as ring-width increases.

Despite their positive association, ring-width and wood density responded to different climatic parameters (Olano et al., 2023). The ring-width of the diffuse-porous beech was negatively related to high temperatures during July and low precipitation during June (Fig. 2), indicating that the growth of this species is constrained by summer drought (Fig. S2) (van der Werf et al., 2007; Leuschner, 2020; Martinez del Castillo et al., 2022), probably due to its dependence on shallow water sources (Fabiani et al., 2021; Kahmen et al., 2022). Year-to-year variation of wood density of beech is also controlled by climate variability (Skomarkova et al., 2006; Peters et al., 2020; Bytebier et al., 2022), and our results point to the importance of climate conditions at the beginning of the growing season before leaf unfolding and cambium reactivation (van der Werf et al., 2007; Čufar et al., 2008). Mean vessel area in beech has been found to depend on water availability during the expansion phase (Olano et al., 2022). So that, high temperatures and low precipitation during March lead to the formation of narrower vessels and, therefore, denser wood (Fig. 4). In central Europe, it has been found that wood density increases with the increase of June-July temperatures (Skomarkova et al., 2006; Peters et al., 2020; Bytebier et al., 2022), but it also depends on spring and summer precipitation (Peters et al., 2020; Bytebier et al., 2022). It is possible that warm and dry springs favour an early start of the growing season enhancing photosynthesis and wood formation (Peters et al., 2020). Additionally, beech seems to be able to resume growth after summer drought if the climate is favourable (van der Werf et al., 2007) potentially increasing the formation of latewood and thus increasing wood density (Peters et al., 2020). It is less clear why cold and dry conditions during the previous autumn increase wood density, but they could lead to an increase in respiration, reducing the non-structural carbohydrate pools and leading to less dense wood formed by cells with thin walls the following spring and summer.

In contrast, the growth of oak seems to be less dependent on summer precipitation and temperatures than that of beech (Fig. 2), thus pointing to the lower impact of summer drought (Fig. S2) in line with previous studies comparing both species (Scharnweber et al., 2013; Vitasse et al., 2019; Vanhellemont et al., 2019; Meyer et al., 2020; Enderle et al., 2024). Instead, oak growth showed a greater dependence on conditions at the start of the growing season, which is likely explained by the high priority of vessel formation, starting before bud break, in ring-porous species (van der Werf et al., 2007). Xylem formation in ring-porous species like *Q. robur* also depends on non-structural carbohydrates stored in sapwood ray parenchyma (Pérez-de-Lis et al., 2016). In addition, oak trees are able to extract water from deep sources (Ripullone et al., 2020; Fabiani et al., 2022; Kahmen et al., 2022), which allows them to maintain high photosynthetic rates and stomatal conductance during water shortage (Raftoyannis and Radoglou, 2002). This strategy enables high water transport capacity and physiological activity during the growing season (van der Werf et al., 2007). The ring-porous oak forms large earlywood vessels in early spring and then develops latewood consisting of small-lumen vessels, but spring-summer temperatures may modify latewood anatomy (Guada et al., 2019). This could explain why high minimum temperatures in May and July lead to thicker vessel and fibre walls and smaller latewood vessel lumen area, consequently, increasing wood density. In D oak trees, wetter April conditions could be associated to higher cloudiness and lower radiation

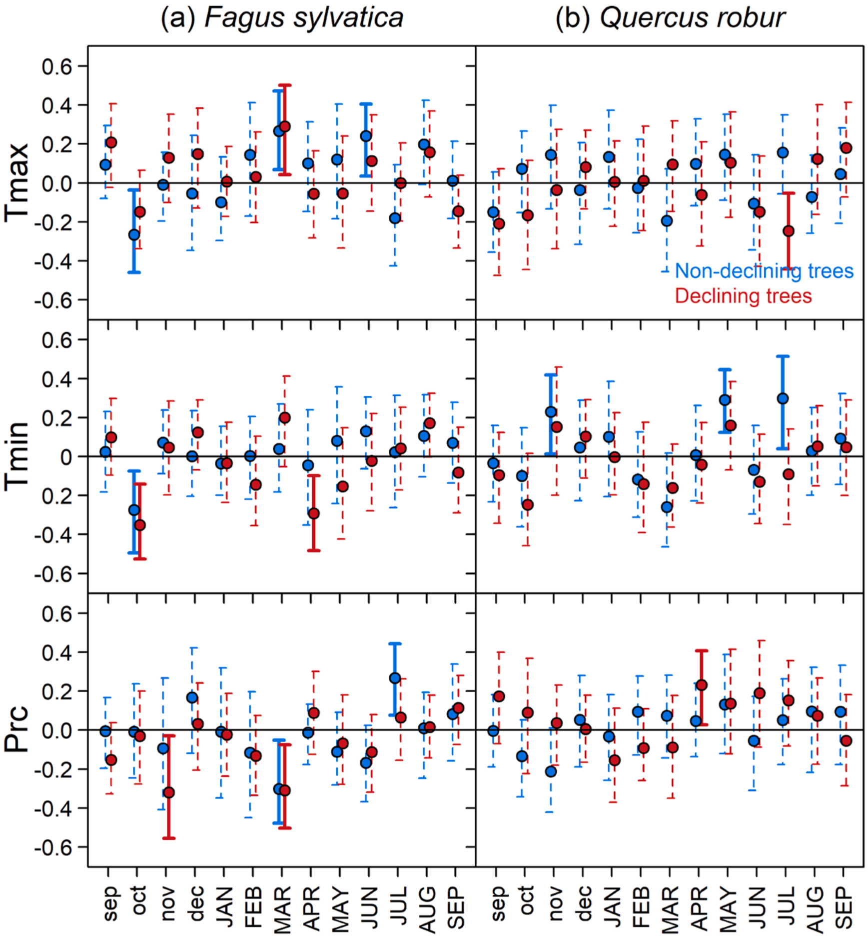

Fig. 4. Bootstrapped correlations between residual ring-density indices (RDIres) and monthly maximum temperature (Tmax), minimum temperature (Tmin) and precipitation (Prc) European beech (*Fagus sylvatica*, **a**) and pedunculate oak (*Quercus robur*, **b**). Symbols with continuous error bars are significant ($p < 0.05$).

levels, thus reducing photosynthetic rates and earlywood vessel expansion, or enhance cambium activity and latewood production in summer, thus increasing wood density.

However, neither ring-width chronologies nor density profiles support a susceptibility of oak to drought in the studied forest (Figs. S2 and S3). Variability of both growth and density seems to be controlled by minimum temperatures during the previous winter and the summer while precipitation effects seem to be restricted to D trees (Figs. 2 and 4). The negative effect of minimum temperatures on oak growth is expected due to the impact of cold spells and their potential interactions with summer water shortage (Rozas, 2005; Helama et al., 2009; Matisons et al., 2013). Collectively, these results suggest that the studied oak site is not water limited and that temperatures control both ring-width and density variability. The causes leading to oak decline appears to be complex and depend on the interaction of multiple factors (Losseau et al., 2020; Macháčová et al., 2022; Kowsari and Karimi, 2023), and, unfortunately, density profiles do not allow attributing potential drivers of oak dieback.

We additionally assessed the potential of resistography to detect differences between D and ND trees in the two species. Resistance to penetration is being widely embraced for commercial wood quality assessment due to its speed and cost-effectiveness (Gao et al., 2017), so exploring its ability to identify growth decline may improve current tools for dieback diagnosis. We found that the resistance drilling increased as moving from the bark to the pith (Fig. 5) in line with other studies due to increasing friction as the needle is inserted into the stem (Arnič et al., 2022). While tree vigour classes of beech did not present differences in their resistograph profiles, D oak trees showed lower resistance drilling than ND trees for the first 3 cm of sapwood, that includes the last *ca.* 20–30 years. We also found that trees with larger growth presented less resistance to penetration which contradicts the increase in wood density as tree ring-width increases. However, it is important to note that these analyses were obtained at the individual level thus suggesting that individuals with higher growth rates present softer wood which is in line with a reduction in density as trees grow faster (Chave et al., 2009; but see Fajardo, 2018).

The findings of this study can be useful to outline some recommendations on the applicability of the different indicators used in this study to identify forest dieback before canopy shows symptoms. Divergence between vigour classes in radial growth patterns was observed despite species and site, pointing to tree ring width studies as an effective method for anticipating impending tree mortality (Cailleret et al., 2017). Previous studies have reported differences in wood density prior to growth (López et al., 2021), however our results are less conclusive and show that the sensitivity of this indicator to dieback depends on other factors (e.g., wood anatomy, growth patterns). Finally, non-destructive measures of resistance drilling density are promising for detecting dieback because of the advantages in terms of time, costs and ease of interpreting the outcomes, although further research is required to fully unravel the potential biases related to the measurement devices and their setup parameters (Fundova et al., 2018; Gendvilas et al., 2024).

5. Conclusions

Altogether, our results support the use of tree-rings as proxy to differentiate between declining and non-declining trees and to attribute

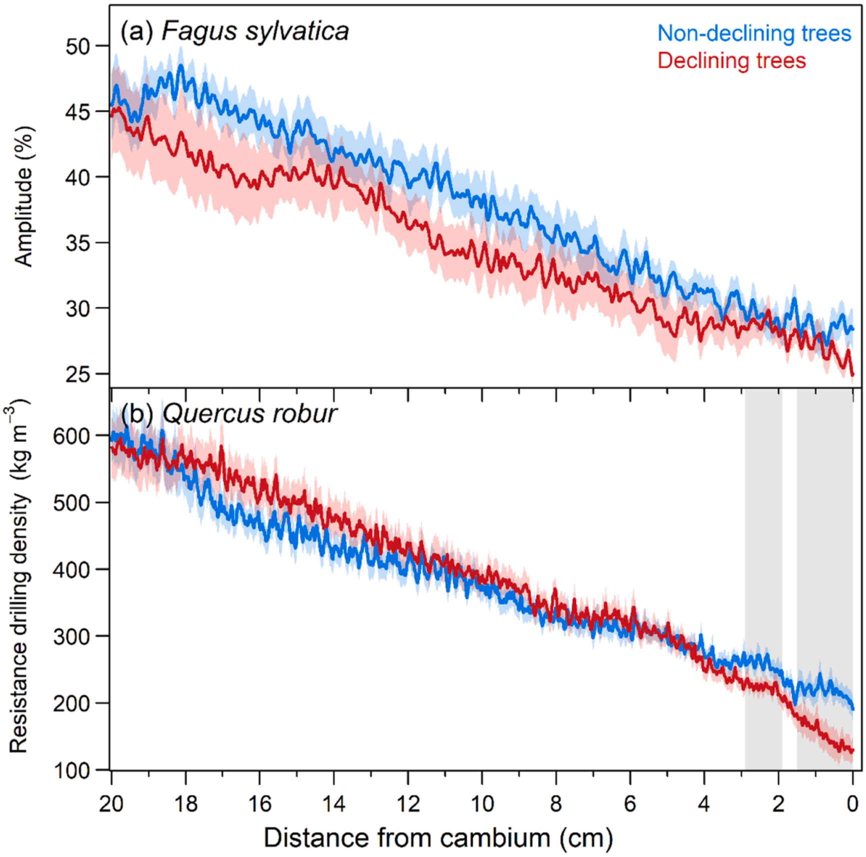

Fig. 5. Resistance drilling profiles of non-declining (blue) and declining (red) trees in the European beech (*Fagus* sylvatica, **a**) and pedunculate oak (*Quercus robur*, **b**) forests. Solid lines represent the means and shaded areas around them the standard error of the mean. The grey filled areas indicate the periods when wood density of tree vigour classes significantly ($p < 0.05$) differed according to Wilcoxon rank- sum tests. Different measurements of resistance drilling are provided due to the different devices used in each species. Note that the *x*-axes scale is inverted to coincide with the general direction of increasing time from left to right.

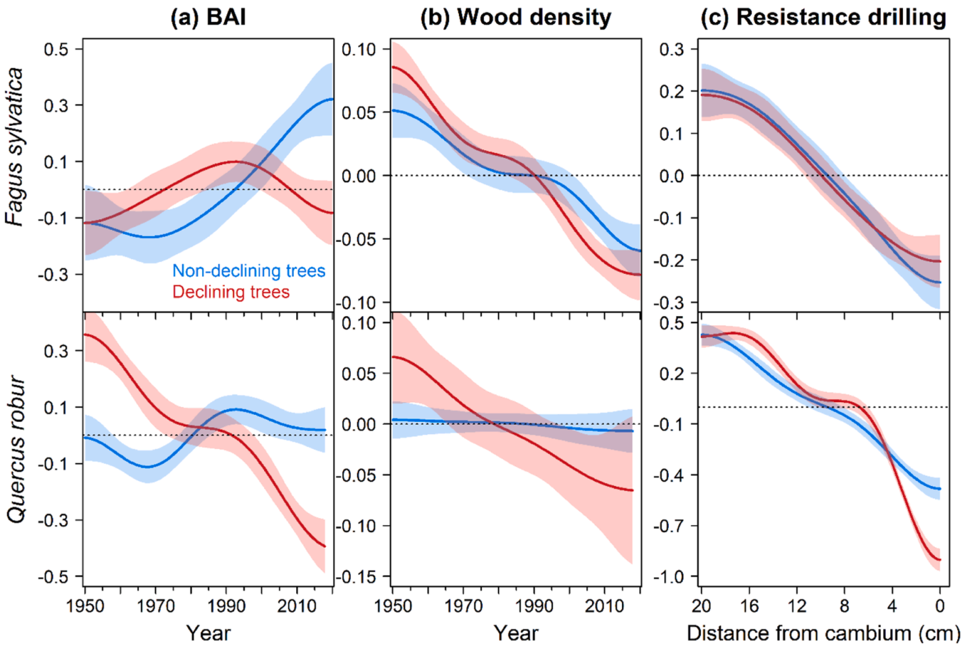

Fig. 6. Long-term trends of basal area increment (BAI, **a**), wood density (**b**) and resistance drilling (**c**) of non-declining (blue bands) and declining (red bands) European beech (*Fagus sylvatica*, upper panels) and pedunculate oak (*Quercus robur*, right panels) individuals according to GAMMs (see Table 3). The line represents the effect and the shaded area the standard errors. Note that in (c) the *x*-axis scale is inverted to coincide with the general direction of increasing time from left to right.

Table 3
Generalized additive mixed-models (GAMMs) of radial growth (BAI), wood density and resistance drilling for each study species. For the linear terms, the *t* statistic is shown, whereas for parameters modelled with spline functions the *F* values are shown (effective degrees of freedom –*edf*– are given between parentheses). The R^2 associated with each model is presented. Significance levels: $p < 0.05$ *, $p < 0.01$ * *, $p < 0.001$ * **. Note that in resistance drilling models, Year variable is substituted by Depth (i.e., distance from the cambium).

		BAI	Wood density	Resistance drilling
Fagus sylvatica	*Linear terms*			
	Vigour class (ND)	0.956	0.055	1.630
	Spline			
	Year * class (ND)	9.681 (2.986) * **	14.05 (3.298)* **	33.74 (3.402) * **
	Year * class (D)	2.637 (2.667) * *	41.71 (3.628)* **	27.03 (3.503) * **
	DBH	3.160 (2.454) * **	0.373 (0.872)	1.656 (2.039)*
	R^2	0.228	0.257	0.415
Quercus robur	*Linear terms*			
	Vigour class (ND)	5.004 * **	2.046 *	1.949 *
	Spline			
	Year * class (ND)	4.355 (3.186) * **	0.129 (0.407)	129.9 (3.840) * **
	Year * class (D)	34.55 (3.604) * **	2.851 (2.063)* **	275.1 (3.951) * **
	DBH	3.416 (2.863) * *	1.044 (1.720)	2.254 (2.099) * *
	R^2	0.587	0.148	0.675

Variables' abbreviations: BAI, basal area increment, ND and D, non-declining and declining trees, respectively (vigour classes), DBH, diameter at breast height.

Table 4
Linear mixed-effects models characterizing the relationship between residual ring-width indices (RWIres, response variable) and residual ring-density indices (RDIres, predictor variable) as a function of the tree vigour class of the study species during the period 1950–2019. For each variable, the *F*-statistic and its associated *p*-value are shown.

	Fagus sylvatica		***Quercus robur***	
	F-statistic	*p*-value	*F*-statistic	*p*-value
RDIres	34.021	< 0.001	9.189	0.002
Vigour class	1.067	0.302	0.258	0.611
RDIres x class	1.074	0.300	0.267	0.605

potential mortality causes (Camarero et al., 2015; Cailleret et al., 2017; DeSoto et al., 2020). Our results support the use of wood densitometry profiles to assess the influence of climate parameters in the wood characteristics of hardwood species, although we only found clear evidence to separate tree vigour classes in ring-porous pedunculate oak. Climate variability during the early growing season controls wood density in beech, while factors influencing wood density in oak were less evident. Our results concur on the high susceptibility to summer drought of European beech. In a scenario in which the length of the growing season is retracted and water scarcity will increase due to warming (Hammond et al., 2022, Rahmati et al., 2023), mortality events may continue in drought limited forests as the one studied here. However, discerning the causes leading to oak decline in the studied forest remains challenging and further investigations should consider the potential influence of microsite conditions which are important in seasonally waterlogged sites (Skiadaresis et al., 2019).

Funding sources

This research was partially funded by the EFA337/19 POCTEFA ACCLIMAFOR 2019–2022 project. AG was supported by the "Ramón y Cajal" Program of the Spanish MICINN under Grant RyC2020–030647-I, and by CSIC under grant PIE-20223AT003. This research was funded by the Spanish Science and Innovation Ministry (projects PID2021–123675OB-C43 and TED2021–129770B-C21).

CRediT authorship contribution statement

Camarero J. Julio: Writing – review & editing, Project administration, Methodology, Funding acquisition, Conceptualization. **Valeriano Cristina:** Writing – review & editing, Methodology. **Cantero Alejandro:** Writing – review & editing, Methodology, Funding acquisition. **Colangelo Michele:** Writing – review & editing, Methodology. **Gonzalez de Andrés Ester:** Writing – review & editing, Writing – original draft, Visualization, Formal analysis, Data curation. **Gazol Antonio:** Writing – review & editing, Writing – original draft, Project administration, Methodology, Funding acquisition, Data curation.

Declaration of Competing Interest

The authors declare the following financial interests/personal relationships which may be considered as potential competing interests:J. Julio Camarero reports financial support was provided by European Commission. Antonio Gazol reports financial support was provided by Spain Ministry of Science and Innovation. Antonio Gazol reports financial support was provided by Spanish Scientific Research Council. If there are other authors, they declare that they have no known competing financial interests or personal relationships that could have appeared to influence the work reported in this paper

Appendix A. Supporting information

Supplementary data associated with this article can be found in the online version at doi:10.1016/j.dendro.2025.126300.

Data availability

Data will be made available on request.

References

Allen, C.D., Breshears, D.D., McDowell, N.G., 2015. On underestimation of global vulnerability to tree mortality and forest die-off from hotter drought in the Anthropocene. Ecosphere 6, 1–50. https://doi.org/10.1890/ES15-00203.1.

Allen, C.D., Macalady, A.K., Chenchouni, H., Bachelet, D., McDowell, N., Vennetier, M., Kitzberger, T., Rigling, A., Breshears, D.D., Hogg, E.H., et al., 2010. A global overview of drought and heat-induced tree mortality reveals emerging climate change risks for forests. For. Ecol. Manag. 259, 660–684. https://doi.org/10.1016/j.foreco.2009.09.001.

Arnič, D., Krajnc, L., Gričar, J., Prislan, P., 2022. Relationships between wood-anatomical features and resistance drilling density in Norway spruce and European beech. Front. Plant Sci. 13, 872950. https://doi.org/10.3389/fpls.2022.872950.

Bergès, L., Nepveu, G., Franc, A., 2008. Effects of ecological factors on radial growth and wood density components of sessile oak (*Quercus petraea* Liebl.) in Northern France. For. Ecol. Manag. 255, 567–579. https://doi.org/10.1016/j.foreco.2007.09.027.

Bontemps, J.D., Gelhaye, P., Nepveu, G., Hervé, J.C., 2013. When tree rings behave like foam: moderate historical decrease in the mean ring density of common beech paralleling a strong historical growth increase. Ann. For. Sci. 70, 329–343. https://doi.org/10.1007/s13595-013-0263-2.

Bose, A.K., Scherrer, D., Camarero, J.J., Ziche, D., Babst, F., Bigler, C., Bolte, A., Dorado-Liñán, I., Etzold, S., Fonti, P., et al., 2021. Climate sensitivity and drought seasonality determine post-drought growth recovery of *Quercus petraea* and *Quercus robur* in Europe. Sci. Total Environ. 784, 147222. https://doi.org/10.1016/j.scitotenv.2021.147222.

Bytebier, J., De Mil, T., Vanhellemont, M., Verheyen, K., Haneca, K., Van den Bulcke, J., 2022. Linking wood density records of common beech (*Fagus sylvatica* L.) with temperature and precipitation variability from a temperate lowland site. Dendrochronologia 76, 126018. https://doi.org/10.1016/j.dendro.2022.126018.

Cailleret, M., Jansen, S., Robert, E.M., DeSoto, L., Aakala, T., Antos, J.A., Beikircher, B., Bigler, C., Bugmann, H., Caccianiga, M., et al., 2017. A synthesis of radial growth patterns preceding tree mortality. Glob. Change Biol. 23, 1675–1690. https://doi.org/10.1111/gcb.13535.

Camarero, J.J., Colangelo, M., Gazol, A., Azorín-Molina, C., 2021. Drought and cold spells trigger dieback of temperate oak and beech forests in northern Spain. Dendrochronologia 66, 125812. https://doi.org/10.1016/j.dendro.2021.125812.

Camarero, J.J., Gazol, A., Sangüesa-Barreda, G., Cantero, A., Sánchez-Salguero, R., Sánchez-Miranda, A., Granda, E., Serra-Maluquer, S., Ibáñez, R., 2018. Forest growth responses to drought at short-and long-term scales in Spain: squeezing the stress memory from tree rings. Front. Ecol. Evol. 6, 9. https://doi.org/10.3389/fevo.2018.00009.

Camarero, J.J., Gazol, A., Sangüesa-Barreda, G., Oliva, J., Vicente-Serrano, S.M., 2015. To die or not to die: early warnings of tree dieback in response to a severe drought. J. Ecol. 103, 44–57. https://doi.org/10.1111/1365-2745.12295.

Chave, J., Coomes, D., Jansen, S., Lewis, S.L., Swenson, N.G., Zanne, A.E., 2009. Towards a worldwide wood economics spectrum. Ecol. Lett. 12, 351–366. https://doi.org/10.1111/j.1461-0248.2009.01285.x.

Colangelo, M., Camarero, J.J., Battipaglia, G., Borghetti, M., De Micco, V., Gentilesca, T., Ripullone, F., 2017. A multi-proxy assessment of dieback causes in a Mediterranean oak species. Tree Physiol. 37, 617–631. https://doi.org/10.1093/treephys/tpx002.

Cook, E.R., Kairiukstis, L.A., 1990. Methods of Dendrochronology. Applications in the Environmental Sciences. International Institute for Applied Systems Analysis. Kluwer Academic Publishers, Dordrecht, p. 394. https://doi.org/10.1007/978-94-015-7879-0.

Cornes, R., van der Schrier, G., van den Besselaar, E.J.M., Jones, P.D., 2018. An ensemble version of the E-OBS temperature and precipitation datasets. Geophys. Res. Atmos, 123, 9391–9409. https://doi.org/10.1029/2017JD028200.

Čufar, K., Prislan, P., de Luis, M., Gričar, J., 2008. Tree-ring variation, wood formation and phenology of beech (*Fagus sylvatica*) from a representative site in Slovenia, SE Central Europe. Trees 22, 749–758. https://doi.org/10.1007/s00468-008-0235-6.

Delpierre, N., Berveiller, D., Granda, E., Dufrêne, E., 2016. Wood phenology, not carbon input, controls the interannual variability of wood growth in a temperate oak forest. N. Phytol. 210, 459–470. https://doi.org/10.1111/nph.13771.

van der Werf, G.W., Sass-Klaassen, U.G., Mohren, G.M.J., 2007. The impact of the 2003 summer drought on the intra-annual growth pattern of beech (*Fagus sylvatica* L.) and oak (*Quercus robur* L.) on a dry site in the Netherlands. Dendrochronologia 25, 103–112. https://doi.org/10.1016/j.dendro.2007.03.004.

DeSoto, L., Cailleret, M., Sterck, F., Jansen, S., Kramer, K., Robert, E.M., Aakala, T., Amoroso, M.M., Bigler, C., Camarero, J.J., Čufar, K., et al., 2020. Low growth resilience to drought is related to future mortality risk in trees. Nat. Commun. 11, 545. https://doi.org/10.1038/s41467-020-14300-5.

Diaconu, D., Wassenberg, M., Spiecker, H., 2016. Variability of European beech wood density as influenced by interactions between tree-ring growth and aspect. For. Ecosyst. 3, 1–9. https://doi.org/10.1186/s40663-016-0065-8.

Drobyshev, I., Linderson, H., Sonesson, K., 2007. Temporal mortality pattern of pedunculate oaks in southern Sweden. Dendrochronologia 24, 97–108. https://doi.org/10.1016/j.dendro.2006.10.004.

Dyderski, M.K., Paź, S., Frelich, L.E., Jagodziński, A.M., 2018. How much does climate change threaten European forest tree species distributions? Glob. Change Biol. 24, 1150–1163. https://doi.org/10.1111/gcb.13925.

Eaton, E., Caudullo, G., Oliveira, S., de Rigo, D., 2016. *Quercus robur* and *Quercus petraea* in Europe: distribution, habitat, usage and threats. In: San-Miguel-Ayanz, J., de Rigo, D., Caudullo, G., Houston Durrant, T., Mauri, A. (Eds.), European Atlas of Forest Tree Species. Publ. Off. EU, Luxembourg pp. e01c6df.

Enderle, L., Gribbe, S., Muffler, L., Weigel, R., Hertel, D., Leuschner, C., 2024. A warmer climate impairs the growth performance of Central Europe's major timber species in lowland regions. Sci. Total Environ. 941, 173665. https://doi.org/10.1016/j.scitotenv.2024.173665.

Fabiani, G., Schoppach, R., Penna, D., Klaus, J., 2022. Transpiration patterns and water use strategies of beech and oak trees along a hillslope. Ecohydrology 15, e2382. https://doi.org/10.1002/eco.2382.

Fajardo, A., 2018. Insights into intraspecific wood density variation and its relationship to growth, height and elevation in a treeline species. Plant Biol. 20, 456–464. https://doi.org/10.1111/plb.12701.

Frei, E.R., Gossner, M.M., Vitasse, Y., Queloz, V., Dubach, V., Gessler, A., Ginzler, C., Hagedorn, F., Meusburger, K., Moor, M., Samblás Vives, E., Rigling, A., Uitentuis, I., von Arx, G., Wohlgemuth, T., 2022. European beech dieback after premature leaf senescence during the 2018 drought in northern Switzerland. Plant Biol. 24, 1132–1145. https://doi.org/10.1111/plb.13467.

Fritts, H.C., 2001. Tree rings and climate. Blackburn Press, p. 567.

Fundova, I., Funda, T., Wu, H.X., 2018. Non-destructive wood density assessment of Scots pine (*Pinus sylvestris* L.) using Resistograph and Pilodyn. PLoS One 13, e0204518. https://doi.org/10.1371/journal.pone.0204518.

Gao, S., Wang, X., Wiemann, M.C., Brashaw, B.K., Ross, R.J., Wang, L., 2017. A critical analysis of methods for rapid and nondestructive determination of wood density in standing trees. Ann. For. Sci. 74, 27. https://doi.org/10.1007/s13595-017-0623-4.

Gauthey, A., Kahmen, A., Limousin, J.M., Vilagrosa, A., Didion-Gency, M., Mas, E., Milano, A., Tunas, A., Grossiord, C., 2024. High heat tolerance, evaporative cooling, and stomatal decoupling regulate canopy temperature and their safety margins in three European oak species. Glob. Change Biol. 30, e17439. https://doi.org/10.1111/gcb.17439.

Gendvilas, V., Downes, G.M., Lausberg, M., Harrington, J.J., Lee, D.J., 2024. Predicting wood density using resistance drilling: the effect of varying feed speed and RPM. Forests 15, 579. https://doi.org/10.3390/f15040579.

Giberti, G.S., von Arx, G., Giovannelli, A., du Toit, B., Unterholzner, L., Bielak, K., Wellstein, C., 2023. The admixture of *Quercus* sp. in *Pinus sylvestris* stands influences wood anatomical trait responses to climatic variability and drought events. Front. Plant Sci. 14, 1213814. https://doi.org/10.3389/fpls.2023.1213814.

Gričar, J., De Luis, M., Hafner, P., Levanič, T., 2013. Anatomical characteristics and hydrologic signals in tree-rings of oaks (*Quercus robur* L.). Trees 27, 1669–1680. https://doi.org/10.1007/s00468-013-0914-9.

Grossiord, C., Buckley, T.N., Cernusak, L.A., Novick, K.A., Poulter, B., Siegwolf, R.T., Sperry, J.S., McDowell, N.G., 2020. Plant responses to rising vapor pressure deficit. N. Phytol. 226, 1550–1566. https://doi.org/10.1111/nph.16485.

Guada, G., Vázquez-Ruiz, R.A., García-González, I., 2019. Response patterns of xylem and leaf phenology to temperature at the southwestern distribution boundary of *Quercus robur*: A multi-spatial study. Agric. For. Meteorol. 269–270, 46–56. https://doi.org/10.1016/j.agrformet.2019.02.001.

Hammond, W.M., Williams, A.P., Abatzoglou, J.T., Adams, H.D., Klein, T., López, R., Sáenz-Romero, C., Hartmann, H., Breshears, D.D., Allen, C.D., 2022. Global field observations of tree die-off reveal hotter-drought fingerprint for Earth's forests. Nat. Commun. 13, 1761. https://doi.org/10.1038/s41467-022-29289-2.

Hartmann, H., Bastos, A., Das, A.J., Esquivel-Muelbert, A., Hammond, W.M., Martínez-Vilalta, J., McDowell, N.G., Powers, J.S., Pugh, T.A.M., Ruthrof, K.X., Allen, C.D., 2022. Climate change risks to global forest health: emergence of unexpected events of elevated tree mortality worldwide. Annu. Rev. Plant Biol. 73, 673–702. https://doi.org/10.1146/annurev-arplant-102820-012804.

Hartmann, H., Moura, C.F., Anderegg, W.R., Ruehr, N.K., Salmon, Y., Allen, C.D., Arndt, S.K., Breshears, D.D., Davi, H., Galbraith, D., Ruthrof, K.X., Wunder, J., Adams, H.D., et al., 2018. Research frontiers for improving our understanding of drought-induced tree and forest mortality. N. Phytol. 218, 15–28. https://doi.org/10.1111/nph.15048.

Helama, S., Läänelaid, A., Raisio, J., Tuomenvirta, H., 2009. Oak decline in Helsinki portrayed by tree-rings, climate and soil data. Plant Soil 319, 163–174. https://doi.org/10.1007/s11104-008-9858-z.

Houston Durrant, T., de Rigo, D., Caudullo, G., 2016. *Fagus sylvatica* and other beeches in Europe: distribution, habitat, usage and threats. In: San-Miguel-Ayanz, J., de Rigo, D., Caudullo, G., Houston Durrant, T., Mauri, A. (Eds.), European Atlas of Forest Tree Species. Publ. Off. EU, Luxembourg pp. e012b90+.

Jiang, Y., Marchand, W., Rydval, M., Matula, R., Janda, P., Begović, K., Thom, D., Fruleux, A., Buechling, A., Pavlin, J., Nogueira, J., et al., 2024. Drought resistance of major tree species in the Czech Republic. Agric. For. Meteorol. 348, 109933. https://doi.org/10.1016/j.agrformet.2024.109933.

Kahmen, A., Basler, D., Hoch, G., Link, R.M., Schuldt, B., Zahnd, C., Arend, M., 2022. Root water uptake depth determines the hydraulic vulnerability of temperate European tree species during the extreme 2018 drought. Plant Biol. 24, 1224–1239. https://doi.org/10.1111/plb.13476.

Kattge, J., Bönisch, G., Díaz, S., Lavorel, S., Prentice, I.C., Leadley, P., Tautenhahn, S., Werner, G.D.A., Aakala, T., Abedi, M., Acosta, A.T.R., Adamidis, G.C., Adamson, K., et al., 2020. TRY plant trait database –enhanced coverage and open access. Glob. Change Biol. 26, 119–188. https://doi.org/10.1111/gcb.14904.

Klein, T., 2014. The variability of stomatal sensitivity to leaf water potential across tree species indicates a continuum between isohydric and anisohydric behaviours. Funct. Ecol. 28, 1313–1320. https://doi.org/10.1111/1365-2435.12289.

Kowsari, M., Karimi, E., 2023. A review on oak decline: The global situation, causative factors, and new research approaches. For. Syst. 32, eR01. https://doi.org/10.5424/fs/2023323-20265.

Lenth, R., 2023. _emmeans: Estimated Marginal Means, aka Least-Squares Means_. R package version 1.8.9, <⟨https://CRAN.R-project.org/package=emmeans⟩>

Leuschner, C., 2020. Drought response of European beech (*Fagus sylvatica* L.)–A review. PPEES 47, 125576. https://doi.org/10.1016/j.ppees.2020.125576.

López, R., Cano, F.J., Rodríguez-Calcerrada, J., Sangüesa-Barreda, G., Gazol, A., Camarero, J.J., Rozenberg, P., Gil, L., 2021. Tree-ring density and carbon isotope composition are early-warning signals of drought-induced mortality in the drought tolerant Canary Island pine. Agric. For. Meteorol. 310, 108634. https://doi.org/10.1016/j.agrformet.2021.108634.

Losseau, J., Jonard, M., Vincke, C., 2020. Pedunculate oak decline in southern Belgium: a long-term process highlighting the complex interplay among drought, winter frost, biotic attacks, and masting. Can. J. For. Res. 50, 380–389. https://doi.org/10.1139/cjfr-2019-0341.

Macháčová, M., Nakládal, O., Samek, M., Baťa, D., Zumr, V., Pešková, V., 2022. Oak decline caused by biotic and abiotic factors in Central Europe: a case study from the Czech Republic. Forests 13, 1223. https://doi.org/10.3390/f13081223.

Martinez del Castillo, E., Zang, C.S., Buras, A., Hacket-Pain, A., Esper, J., Serrano-Notivoli, R., Hartl, C., Weigel, R., Klesse, S., Resco de Dios, V., Scharnweber, T., Dorado-Liñán, I., 2022. Climate-change-driven growth decline of European beech forests. Commun. Biol. 5, 163. https://doi.org/10.1038/s42003-022-03107-3.

Matisons, R., Elferts, D., Brūmelis, G., 2013. Possible signs of growth decline of pedunculate oak in Latvia during 1980–2009 in tree-ring width and vessel size. Balt 19, 137–142.

Maxwell, R.S., Larsson, L.-A., 2021. Measuring tree-ring widths using the CooRecorder software application. Dendrochronologia 67, 125841. https://doi.org/10.1016/j.dendro.2021.125841.

Mehtätalo, L., Comas, C., Pukkala, T., Palahí, M., 2011. Combining a predicted diameter distribution with an estimate based on a small sample of diameters. Can. J. For. Res. 41, 750–762. https://doi.org/10.1139/x11-008.

Meyer, B.F., Buras, A., Rammig, A., Zang, C.S., 2020. Higher susceptibility of beech to drought in comparison to oak. Dendrochronologia 64, 125780. https://doi.org/10.1016/j.dendro.2020.125780.

Minikaev, D., Ventura, M., Tonon, G., Uhl, E., Ravaioli, D., Jankowski, P.A., Wellstein, C., 2024. Canopy nitrogen application effects on *Quercus petraea* L. and *Fagus sylvatica* L. ring width and wood density. Eur. J. For. Res. https://doi.org/10.1007/s10342-024-01693-x.

Olano, J.M., Hernández-Alonso, H., Sangüesa-Barreda, G., Rozas, V., García-Cervigón, A. I., García-Hidalgo, M., 2022. Disparate response to water limitation for vessel area and secondary growth along *Fagus sylvatica* southwestern distribution range. Agric. For. Meteorol. 323, 109082. https://doi.org/10.1016/j.agrformet.2022.109082.

Olano, J.M., Sangüesa-Barreda, G., García-López, M.A., García-Hidalgo, M., Rozas, V., García-Cervigón, A.I., Delgado-Huertas, A., Hernández-Alonso, H., 2023. Water use efficiency and climate legacies dominate beech growth at its rear edge. J. Ecol. 111, 2160–2171. https://doi.org/10.1111/1365-2745.14164.

Pérez-de-Lis, G., García-González, I., Rozas, V., Olano, J.M., 2016. Feedbacks between earlywood anatomy and non-structural carbohydrates affect spring phenology and wood production in ring-porous oaks. Biogeosciences 13, 5499–5510.

Peters, R.L., von Arx, G., Nievergelt, D., Ibrom, A., Stillhard, J., Trotsiuk, V., Mazurkiewicz, A., Babst, F., 2020. Axial changes in wood functional traits have limited net effects on stem biomass increment in European beech (*Fagus sylvatica*). Tree Physiol. 40, 498–510. https://doi.org/10.1093/treephys/tpaa002.

Pretzsch, H., Biber, P., Schütze, G., Kemmerer, J., Uhl, E., 2018. Wood density reduced while wood volume growth accelerated in Central European forests since 1870. For. Ecol. Manag. 429, 589–616. https://doi.org/10.1016/j.foreco.2018.07.045.

Raftoyannis, Y., Radoglou, K., 2002. Physiological responses of beech and sessile oak in a natural mixed stand during a dry summer. Ann. Bot. 89, 723–730. https://doi.org/10.1093/aob/mcf133.

Rahmati, M., Graf, A., Poppe Terán, C., Amelung, W., Dorigo, W., Franssen, H.J.H., Montzka, C., Or, D., Sprenger, M., Vanderborght, J., Verhoest, N.E.C., Vereecken, H., 2023. Continuous increase in evaporative demand shortened the growing season of European ecosystems in the last decade. Commun. Earth Environ. 4, 236. https://doi.org/10.1038/s43247-023-00890-7.

Rao, R.V., Aebischer, D.P., Denne, M.P., 1997. Latewood density in relation to wood fibre diameter, wall thickness, and fibre and vessel percentages in *Quercus robur* L. IAWA J. 18, 127–138.

Ripullone, F., Camarero, J.J., Colangelo, M., Voltas, J., 2020. Variation in the access to deep soil water pools explains tree-to-tree differences in drought-triggered dieback of Mediterranean oaks. Tree Physiol. 40, 591–604. https://doi.org/10.1093/treephys/tpaa026.

Rohner, B., Kumar, S., Liechti, K., Gessler, A., Ferretti, M., 2021. Tree vitality indicators revealed a rapid response of beech forests to the 2018 drought. Ecol. Indic. 120, 106903. https://doi.org/10.1016/j.ecolind.2020.106903.

Rozas, V., 2005. Dendrochronology of pedunculate oak (*Quercus robur* L.) in an old-growth pollarded woodland in northern Spain: tree-ring growth responses to climate. Ann. For. Sci. 62, 209–218. https://doi.org/10.1051/forest:2005012.

Rozas, V., García-González, I., 2012. Too wet for oaks? Inter-tree competition and recent persistent wetness predispose oaks to rainfall-induced dieback in Atlantic rainy forest. Glob. Planet. Ch. 94–95, 62–71. https://doi.org/10.1016/j.gloplacha.2012.07.004.

Santiago, L.S., Goldstein, G., Meinzer, F.C., Fisher, J.B., Machado, K., Woodruff, D., Jones, T., 2004. Leaf photosynthetic traits scale with hydraulic conductivity and wood density in Panamian forest canopy trees. Oecolgia 140, 543–550. https://doi.org/10.1007/s00442-004-1624-1.

Scharnweber, T., Manthey, M., Wilmking, M., 2013. Differential radial growth patterns between beech (*Fagus sylvatica* L.) and oak (*Quercus robur* L.) on periodically waterlogged soils. Tree Physiol. 33, 425–437. https://doi.org/10.1093/treephys/tpt020.

Senf, C., Buras, A., Zang, C.S., Rammig, A., Seidl, R., 2020. Excess forest mortality is consistently linked to drought across Europe. Nat. Comm. 11, 6200. https://doi.org/10.1038/s41467-020-19924-1.

Serra-Maluquer, X., Gazol, A., Sangüesa-Barreda, G., Sánchez-Salguero, R., Rozas, V., Colangelo, M., Gutiérrez, E., Camarero, J.J., 2019. Geographically structured growth decline of rear-edge Iberian *Fagus sylvatica* forests after the 1980s shift toward a warmer climate. Ecosystems 22, 1325–1337. https://doi.org/10.1007/s10021-019-00339-z.

Skiadaresis, G., Schwarz, J.A., Bauhus, J., 2019. Groundwater extraction in floodplain forests reduces radial growth and increases summer drought sensitivity of pedunculate oak trees (*Quercus robur* L.). Front. For. Glob. Change 2, 5. https://doi.org/10.3389/ffgc.2019.00005.

Skomarkova, M.V., Vaganov, E.A., Mund, M., Knohl, A., Linke, P., Boerner, A., Schulze, E.D., 2006. Inter-annual and seasonal variability of radial growth, wood density and carbon isotope ratios in tree rings of beech (*Fagus sylvatica*) growing in Germany and Italy. Trees 20, 571–586. https://doi.org/10.1007/s00468-006-0072-4.

Soheili, F., Woodward, S., Almasi, I., Abdul-Hamid, H., Naji, H.R., 2021. Variations in wood density, annual ring width and vessel properties of *Quercus brantii* affected by crown dieback. Forests 12, 642. https://doi.org/10.3390/f12050642.

Süßel, F., Brüggemann, W., 2021. Properties of secondary xylem of mature oaks in southwest Germany formed after extreme drought stress in summer 2018. Trees For. People 5, 100097. https://doi.org/10.1016/j.tfp.2021.100097.

Toigo, M., Vallet, P., Tuilleras, V., Lebourgeois, F., Rozenberg, P., Perret, S., Courbaud, B., Perot, T., 2015. Species mixture increases the effect of drought on tree ring density, but not on ring width, in *Quercus petraea–Pinus sylvestris* stands. For. Ecol. Manag. 345, 73–82. https://doi.org/10.1016/j.foreco.2015.02.019.

Torresan, C., Hilmers, T., Avdagić, A., Di Giuseppe, E., Klopćić, M., Lévesque, M., Motte, F., Uhl, E., Zlatanov, T., Pretzsch, H., 2024. Changes in tree-ring wood density of European beech (*Fagus sylvatica* L.), silver fir (*Abies alba* Mill.), and Norway spruce (*Picea abies* (L.) H. Karst.) in European mountain forests between 1901 and 2016. Ann. For. Sci. 81, 49. https://doi.org/10.1186/s13595-024-01264-5.

Tulik, M., 2014. The anatomical traits of trunk wood and their relevance to oak (*Quercus robur* L.) vitality. Eur. J. For. Res. 133, 845–855. https://doi.org/10.1007/s10342-014-0801-y.

Vanhellemont, M., Sousa-Silva, R., Maes, S.L., Van den Bulcke, J., Hertzog, L., De Groote, S.R., Van Acker, J., Bonte, D., Martel, A., Lens, L., Verheyen, K., 2019. Distinct growth responses to drought for oak and beech in temperate mixed forests. Sci. Total Environ. 650, 3017–3026. https://doi.org/10.1016/j.scitotenv.2018.10.054.

Vicente-Serrano, S.M., Beguería, S., López-Moreno, J.I., 2010. A multiscalar drought index sensitive to global warming: the standardized precipitation evapotranspiration index. J. Clim. 23, 1696–1718. https://doi.org/10.1175/2009JCLI2909.1.

Vicente-Serrano, S.M., Tomas-Burguera, M., Beguería, S., Reig, F., Latorre, B., Peña-Gallardo, M., Luna, M.Y., Morata, A., González-Hidalgo, J.C., 2017. A high resolution dataset of drought indices for Spain. Data 2, 1–10. https://doi.org/10.3390/data2030022.

Vitasse, Y., Bottero, A., Cailleret, M., Bigler, C., Fonti, P., Gessler, A., Lévesque, M., Rohner, B., Weber, P., Rigling, A., Wohlgemuth, T., 2019. Contrasting resistance and resilience to extreme drought and late spring frost in five major European tree species. Glob. Change Biol. 25, 3781–3792. https://doi.org/10.1111/gcb.14803.

Yin, X.H., Hao, G.Y., Sterck, F., 2023. Ring- and diffuse-porous tree species from a cold temperate forest diverge in stem hydraulic traits, leaf photosynthetic traits, growth rate and altitudinal distribution. Tree Physiol. 43, 722–736. https://doi.org/10.1093/treephys/tpad008.